Journal of Sound and Vibration (1999) **221**(2), 251–272
Article No. jsvi.1998.2013, available online at http://www.idealibrary.com on IDEAL

EFFICIENCY OF A MONOPOLE SOUND SOURCE IN THE VICINITY OF A WATER-LOADED PLATE

C. KAUFFMANN

Delft University of Technology, *Faculty of Technical Mathematics and Informatics*, *P.O. Box* 5031, 2600 *GA Delft*, *The Netherlands*

(*Received* 14 *February* 1997, *and in final form* 29 *September* 1998)

This paper presents numerical results for the power output of a sound source in the vicinity of an elastic structure. The source is a monopole characterized by a constant rate of volume injection. The structure is a thin elastic plate of infinite extent. The coupling of the plate's flexural motion and the acoustic field is taken into account. The acoustic energy emitted by the source is carried away to infinity by acoustic radiation as well as by flexural waves that travel along the plate, accompanied by a coupled, subsonic surface wave in the fluid. For the case of steel plates in water, numerical results have been obtained for the total power delivered by the source as well as for the various power flows involved. The dependence of these results upon two parameters is investigated by extensive numerical calculations. These parameters are: (i) the diffraction or Helmholtz number $k_0 d$, where k_0 is the fluid wavenumber and d is the distance from the source to the plate, and (ii) the ratio of the plate thickness h and d. The power output of the source depends strongly upon the region of interest in this two-parameter space. For $k_0 d \geqslant 1$ the total power output approaches the free field value, but also shows the typical modulation due to the finite distance to the plate. For $h/d \geqslant 0{\cdot}1$ this modulation effect is comparable to that for an infinite rigid wall, while for $h/d \leqslant 0{\cdot}01$ it resembles the effect for a free surface. For $k_0 d < 1$ and $h/d \leqslant k_0 d/20$ the results do not vary with h/d, but the effect of the plate is very close to that for a perfectly compliant surface. In a third regime, i.e., for $0{\cdot}1 \geqslant h/d \geqslant k_0 d/10$, the efficiency of the source is independent of $k_0 h$, but increases strongly with decreasing $k_0 d^2/h$.

1. INTRODUCTION

This paper presents numerical results for the power output of a monopole sound source in the vicinity of a water-loaded plate. The source is characterized by a constant source strength: i.e., its volume velocity is not affected by the type of geometry of the surrounding space or the acoustic properties of the ambient medium. A typical example of such a source is a cavitating ship propeller beneath the aft body of a ship; see e.g., reference [1]. For flat bottom ships like roll-on roll-off container carriers sailing at moderate or high speed—i.e., above the cavitation inception velocity—cavitation volumes of about $1\,\mathrm{m}^3$ have been observed, cf. reference [2], at the suction side of the blades (sheet cavitation) of

0022–460X/99/120251 + 22 $30.00/0

a 6·8 m diameter propeller. This type of cavitation appears on the blades upon entrance of the upper part of the propeller disk and disappears after about a quarter revolution. This phenomenon is hydrodynamically controlled and its acoustical source characteristics (i.e., the rate of volume injection) are not sensitive to variations in the acoustic impedance of the surrounding space.

The acoustical source strength of a cavitating propeller can be determined theoretically: i.e., by numerical prediction of the flow around the propeller, see e.g., reference [3], or experimentally by means of a reciprocity experiment as described by Ten Wolde and De Bruijn [4].

The importance of considering such a source with an elastic structure in its near field lies in the observation that a cavitating propeller is a severe source of sound on board ships. Although other sources like vibrating machinery and main or auxiliary engines can produce considerable noise and vibration levels, their effectiveness in transfer of vibrational energy to the ship's structure has been largely reduced by successful application of resilient mounting systems. Besides, additional measures like the application of sound absorbing material and the construction of floating floors are important for high frequency noise control, but usually fail at low frequencies. Therefore, cavitation noise is still the dominating source of low frequency noise and vibration levels on board ships.

In this paper the various power flows from the source to infinity are investigated for the model problem of a point monopole source at a finite distance from a fluid-loaded plate. Among the extensive literature on fluid-loaded plates, most papers are concerned with the scattering of plane waves by the plate or with the vibration and radiation phenomena of a mechanically driven plate, while relatively few papers deal with the case of a plate irradiated by a point source. Among the latter Krasil'nikov [5] investigated the structure of the far field in the fluid and of the surface wave and its associated plate wave. His analysis, however, is restricted to the low frequency range. Dealing with both classical plate theory as well as thick (Timoshenko–Mindlin) plate theory and assuming that the same fluid is present on both sides of the plate Schmidt [6] studied the power flows from the source to infinity. Schmidt also presented numerical results for wooden and steel plates in air for a wide range of frequencies. His results, however, remain incomplete since he gave no results for steel plates in water, which is a case of considerable practical importance. Moreover, his results are restricted to the case where the point source is located at zero distance from the plate. Finally, Saadat and Filippi [7], using a modified inverse Fourier–Hankel transform representation, derived a series expansion for the far field of both the acoustic pressure and the plate displacement and also presented expressions for the power flows. However, no numerical results were included.

Heckl, in a more qualitative but illuminating study [8] analyzed the excitation of structure-borne sound in simple structures (like membranes, plates and cylindrical shells) placed in the near field of localized hydro-acoustic sources. Although his analysis is restricted to the transmission of energy from the source to the structure, Heckl has provided an important physical explanation for the phenomenon that the structural sound energy can be considerably higher than the

energy radiated by the source under free field conditions. Following remarks by Rayleigh [9], he argued that part of the reactive power in the hydrodynamic near field of the source can be transformed to an active power flow by the action of a resonator or a wave-bearing object.

More recently, for steel plates in water, numerical results for the surface pressure and the plate response directly below the source were obtained by Van Gent *et al*. [10] and by De Bruijn [11, 12]. A comparison with some experimental results was also given by De Bruijn. Most of the results of Van Gent *et al*., however, were restricted to a few, very low frequencies and three values for the plate's thickness ($0{\cdot}02 < k_0 d < 0{\cdot}189$ and $0{\cdot}01 < h/d < 0{\cdot}133$). Their most intriguing result is the ratio of the total pressure to the pressure induced by a rigid wall at the epicenter, i.e., the position on the plate directly below the source, and shows a pressure drop for frequencies in the range 10–100 Hz. De Bruijn presented values for the ratio of the total pressure to the incident pressure at the epicentre for a wider frequency range, 10–500 Hz, but did not vary the plate's thickness. His results include the pressure drop, but also indicate that, for very low frequencies, the pressure rises to values well above the free field reference value. His conclusion that sources may behave quite differently (compared to the free field case) if an elastic structure is placed in its near field, is certainly correct. However, it lacks quantitative information about the conditions on the parameters of interest which this occurs. These authors have raised the question whether the plate behaves like a free surface rather than like a rigid plane. A comparison with the free surface behaviour has not been made, however, since that would require a comparison of the surface velocity instead of the surface pressure. Moreover, this comparison should not be restricted to the epicentre, but should involve an area of several acoustic wavelengths. Since the parameter plane was covered only partly—dimensionless parameters were not used—it is instructive to see where the behaviour of the plate changes from that of a free surface to that of a perfectly rigid wall. Additionally, rather than studying field quantities (surface pressure and plate velocity) the present work is concentrated on the power flows.

The aim of this paper is to clarify the influence of the distance from the source to the plate on the various power flows involved in the fluid-plate system and on the power output of the source. This is done by presenting numerical results for a wide frequency range. All numerical results are obtained for steel plates in water, but cover the full two-dimensional parameter space $0{\cdot}001 \leqslant h/d \leqslant 1{\cdot}0$ and $0{\cdot}01 \leqslant k_0 d \leqslant 10{\cdot}0$, where h is the plate thickness, d is the distance from the source to the plate and k_0 is the wavenumber in the fluid. A physical interpretation is sought by comparing the results to those for a point source in the vicinity of a rigid wall and a free surface.

The paper is organized as follows. In the next section a useful formula is recalled for the power output of a point source in the vicinity of a scattering object. In section 3, the theory is presented and the formulas for the various power flows are derived. Section 4 presents the numerical results and concludes with a discussion of the characteristic features of the solution in the various parts of the parameter space.

2. POWER OUTPUT OF A MONOPOLE SOURCE IN THE VICINITY OF A SCATTERER

In this section a general formula is presented for the power output of a monopole sound source in the vicinity of a scattering object. This formula is due to Schmidt [6] and was derived along classical lines. Despite its simplicity and generality, the formula has not been included as yet in any textbook or reference work on acoustics. Therefore, a short discussion of this formula is given below. For later use and reference it will be applied to the special case of a monopole above a plane, infinite boundary of either zero or infinite normal impedance.

Consider a point monopole of strength q_s, located at position $\underline{x}_s$, radiating sound waves into the domain $D \subset \mathbb{R}^3$ at constant circular frequency ω. The acoustic pressure $p(\underline{x})$ satisfies the Helmholtz equation

$$\{\Delta + k_0^2\} p(\underline{x}) = -q_s \, \delta(\underline{x} - \underline{x}_s), \qquad \underline{x} \in D, \tag{1}$$

where $k_0 = \omega/c_0$ is the acoustic wavenumber and c_0 is the speed of sound. The complex time-harmonic dependence $\exp(-\mathrm{i}\omega t)$ is suppressed throughout.

The geometry of the scattering object is described by its boundary Γ. The boundary condition for p can be written in the general form

$$\alpha p + \beta \frac{\partial p}{\partial n} = 0, \qquad \underline{x} \in \Gamma, \tag{2}$$

where $\underline{n}$ is the unit normal on Γ pointing away from the scattering object, and $\partial/\partial n \equiv \underline{n} \cdot \nabla$. For sound absorbing scatterers, α and β satisfy the condition $\mathrm{Im}\,(\beta/\alpha) < 0$. Equation (2) describes a locally reacting surface by specifying its normal impedance in terms of α and β, which may vary along Γ. For a rigid scatterer $\alpha = 0$ and $\beta = 1$, while for a perfectly compliant or sound soft object $\alpha = 1$ and $\beta = 0$.

If D is unbounded, the Sommerfeld radiation condition should be fulfilled, i.e.,

$$\lim_{s \to \infty} s \left\{ \frac{\partial p}{\partial s} - \mathrm{i} k_0 p(\underline{x}) \right\} = 0, \qquad s = |\underline{x}|. \tag{3}$$

For the present purpose it suffices to write the pressure in the form

$$p(\underline{x}) = p_{inc}(\underline{x}) + p_{scat}(\underline{x}), \qquad \underline{x} \in D, \tag{4}$$

where p_{inc} is the incident pressure radiated by the source if it were placed in free space, and is given by

$$p_{inc}(\underline{x}) = q_s \frac{\exp(\mathrm{i} k_0 R)}{4\pi R}, \qquad R = |\underline{x} - \underline{x}_s|, \tag{5}$$

while p_{scat} represents the pressure due to the presence of the scatterer.

The power output by the source can be evaluated by integrating the power flow through a closed surface Σ containing the source, namely,

$$\Pi = \int\int_{\Sigma} \underline{v} \cdot \underline{I}\, \mathrm{d}S, \tag{6}$$

where $\underline{v}$ is the outward unit normal on Σ and $\underline{I}$ is the acoustic intensity vector defined by $\underline{I} = \frac{1}{2}\mathrm{Re}\,[p\underline{v}^*]$, while $\underline{v}$ is the acoustic velocity perturbation and the asterisk * denotes complex conjugation. If Σ is a sphere of radius ϵ and center $\underline{x}_s$, expression (6) becomes

$$\Pi = \frac{1}{2}\,\mathrm{Re}\left[\int_0^{2\pi} \mathrm{d}\phi \int_0^{\pi} \epsilon^2 \sin\theta\, \mathrm{d}\theta p(\underline{x})\left\{\frac{1}{\rho_0 \mathrm{i}\omega}\frac{\partial p}{\partial R}\right\}^*\right], \tag{7}$$

where p is evaluated at $R = \epsilon$. The linearized momentum equation, i.e., $\underline{v} = (\rho_0 \mathrm{i}\omega)^{-1}\nabla p$ has been used to relate the radial component of $\underline{v}$ to $\partial p/\partial R$. In this expression ρ_0 is the volume density of mass of the fluid. Spherical co-ordinates around $\underline{x}_s$ have been introduced: R is the radius, θ is the polar angle and ϕ is the azimuthal angle. Substitution of equation (4) leads to an expression for Π that consists of four additive terms. It can be shown that for $\epsilon \to 0$ only two terms do not vanish. The first term, which is equal to expression (7) except that p is replaced by p_{inc}, represents the power output of the source in free space. Taking the limit for $\epsilon \to 0$ yields

$$\Pi_\infty = \frac{1}{8\pi}\frac{|q_s|^2}{\rho_0 c_0}. \tag{8}$$

Upon noting that p_{scat} is finite and sufficiently smooth at $\underline{x}_s$, the second non-vanishing term follows. The result is

$$\lim_{\epsilon\to 0}\frac{1}{2}\,\mathrm{Re}\left[\int_0^{2\pi} \mathrm{d}\phi \int_0^{\pi} \epsilon^2 \sin\theta\, \mathrm{d}\theta p_{scat}(\underline{x})\left\{\frac{1}{\rho_0 \mathrm{i}\omega}\frac{\partial p_{inc}}{\partial R}\right\}^*\right]$$

$$= \lim_{\epsilon\to 0}\frac{1}{2}\,\mathrm{Re}\left[\int_0^{2\pi} \mathrm{d}\phi \int_0^{\pi} \sin\theta\, \mathrm{d}\theta \epsilon^2 p_{scat}(\underline{x})\left\{\frac{q_s}{\rho_0 \mathrm{i}\omega}\left(\mathrm{i}k_0 - \frac{1}{\epsilon}\right)\frac{\exp(\mathrm{i}k_0\epsilon)}{4\pi\epsilon}\right\}^*\right]$$

$$= \frac{1}{2\rho_0\omega}\,\mathrm{Re}\,[-\mathrm{i}q_s^* p_{scat}(\underline{x}_s)].$$

Without loss of generality it is assumed that q_s is real and the total power takes the form

$$\Pi = \Pi_\infty + \frac{q_s}{2\rho_0\omega}\,\mathrm{Im}\,[p_{scat}(\underline{x}_s)]. \tag{9}$$

In order to illustrate the use of formula (9) one can consider the case of a point source at distance d above a plane boundary of infinite extent. The normal

impedance is taken infinite or zero, respectively. The method of images gives the scattered field, i.e.,

$$p_{scat}(\underline{x}) = \pm q_s \frac{\exp(\mathrm{i}k_0 R')}{4\pi R'}, \qquad R' = |\underline{x} - \underline{x}_{s'}|, \tag{10}$$

where $\underline{x}_{s'}$ is the position of the image source (at distance d below the plane boundary), while the $\pm$ signs correspond to the perfectly rigid plane and the perfectly compliant surface, respectively. Inserting this expression into equation (9) and using that $|\underline{x}_s - \underline{x}_{s'}| = 2d$ one arrives at the well-known formula, cf. reference [13],

$$\Pi = \Pi_\infty \left[1 \pm \frac{\sin(2k_0 d)}{2k_0 d} \right]. \tag{11}$$

It is noted, however, that this formula was obtained in reference [13] by integrating the directivity of the combined "source–image source" configuration over a hemisphere at infinity.

It is noted that the formula for the power emitted by the source applies equally well to a more general class of scattering objects than those described by equation (2), which describes a locally reacting surface scatterer in terms of its normal impedance. Formula (9) is also valid for volume scatterers consisting of acoustically passive or lossy material. Such scatterers typically show a non-local reaction to an incident wave. In this paper the formula is applied to the case of a thin, elastic plate which is neither a locally reacting surface nor a volume scatterer, but a wave-bearing surface. However, as stated by Schmidt [6] and as is evident from its derivation, the only restriction on the type of scatterer is that p_{scat} is finite and sufficiently smooth at $\underline{x}_s$.

3. THEORY

3.1. GOVERNING EQUATIONS

Consider a perfect acoustic fluid, characterized by its density of mass ρ_0 and speed of sound c_0. The fluid occupies the halfspace $z > 0$. A point monopole source is located on the z-axis at distance d above the plane $z = 0$, where a thin, elastic plate of infinite extent is in continuous contact with the fluid. See Figure 1. The acoustic pressure $p(\underline{x})$ satisfies the Helmholtz equation

$$\{\Delta + k_0^2\} p(\underline{x}) = -q_s \, \delta(\underline{x} - \underline{x}_s), \qquad z > 0, \tag{12}$$

the Neumann condition derived from the continuity of plate and fluid velocities at the plate's surface

$$\frac{\partial p}{\partial z} = \rho_0 \mathrm{i}\omega v(x, y), \qquad -\infty < x, y < \infty, \qquad z = 0, \tag{13}$$

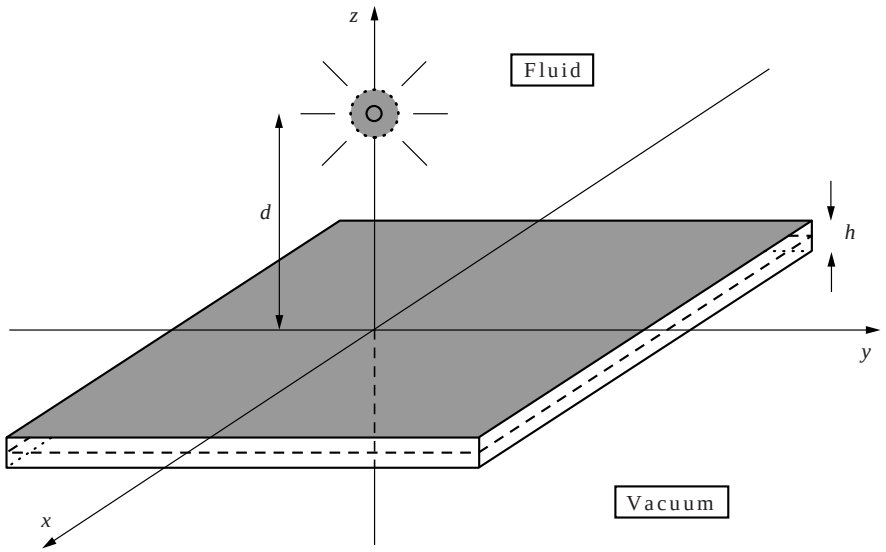

Figure 1. Sketch of problem configuration.

and the Sommerfeld radiation condition (3). According to classical plate theory the out-of-plane flexural vibrations of the plate are governed by

$$D\Delta\Delta u - m\omega^2 u(x, y) = -p(x, y, 0), \qquad -\infty < x, y < \infty, \tag{14}$$

where the right-hand-side represents the acoustic pressure that drives the plate and also accounts for the fluid-loading. In equation (14), $D = Eh^3/12(1 - \nu^2)$ is the bending stiffness, $m = \rho_p h$ is the mass per unit area of the plate, E is Young's modulus, ν is Poisson's ratio, ρ_p is the volume density of mass of the plate and h is the plate thickness. For time-harmonic motions the plate displacement u is related to the plate velocity v by $u = v/-\mathrm{i}\omega$. At infinity, i.e., for $r = (x^2 + y^2)^{1/2} \to \infty$, a radiation condition and a boundedness condition are required to ensure a unique and physically meaningful solution for u.

3.2. ANALYSIS BY FOURIER–HANKEL INTEGRAL TRANSFORMS

Since the configuration shows rotational symmetry around the z-axis the solution will be axisymmetric. Fourier–Hankel integral transformations are used because they are particularly suitable to cope with this type of symmetry.

As a preparatory step the pressure $p(\underline{x})$ is decomposed into three parts as follows:

$$p(\underline{x}) = p_{inc}(\underline{x}) + p_{spec}(\underline{x}) + p_{diff}(\underline{x}). \tag{15}$$

Here $p_{inc} + p_{spec}$ is the solution of the non-homogeneous Helmholtz equation (12) subject to a homogeneous Neumann condition at $z = 0$, while p_{diff} satisfies the homogeneous Helmholtz equation subject to the non-homogeneous Neumann condition (13). p_{inc} is the incident pressure field radiated by the source in free space

and p_{spec} is the specularly reflected part of the pressure which would be present if the plate would be perfectly rigid. p_{inc} and p_{spec} are given by

$$p_{inc}(\underline{x}) = q_s \frac{\exp(\mathrm{i}k_0 R_+)}{4\pi R_+}, \qquad R_+ = \sqrt{r^2 + (z-d)^2}, \tag{16}$$

$$p_{spec}(\underline{x}) = q_s \frac{\exp(\mathrm{i}k_0 R_-)}{4\pi R_-}, \qquad R_- = \sqrt{r^2 + (z+d)^2}. \tag{17}$$

Since the plate is neither rigid nor perfectly compliant p_{diff} represents the pressure field radiated by the vibrations of the plate.

Fourier–Hankel transform pairs are introduced by

$$\tilde{v}(k) = 2\pi \int_0^\infty v(r) J_0(kr) r \, \mathrm{d}r, \tag{18}$$

$$v(r) = \frac{1}{2\pi} \int_{C^+} \tilde{v}(k) J_0(kr) k \, \mathrm{d}k = \frac{1}{4\pi} \int_C \tilde{v}(k) H_0^{(1)}(kr) k \, \mathrm{d}k, \tag{19}$$

where the contour C runs along the real axis in the complex k-plane. Poles located on this contour are accounted for by taking the Cauchy principal value of the integral, while the radiation condition implies that integration along the associated semi-circular paths around these poles must be taken in clockwise direction for poles on the negative real axis and in counterclockwise direction for poles on the positive real axis. The contour C^+ is that part of C that runs along the positive real axis from 0 to ∞. Taking the transforms of equations (15), (12), (13) and (14) and using $\tilde{u} = \tilde{v}/-\mathrm{i}\omega$ yields

$$\tilde{p}(k; z) = \tilde{p}_{inc}(k; z) + \tilde{p}_{spec}(k; z) + \tilde{p}_{diff}(k; z), \tag{20}$$

$$\left\{ \frac{\mathrm{d}^2}{\mathrm{d}z^2} + (k_0^2 - k^2) \right\} \tilde{p}_{diff}(k; z) = 0, \tag{21}$$

$$\frac{\mathrm{d}\tilde{p}_{diff}}{\mathrm{d}z}(k; 0) = \rho_0 \mathrm{i}\omega \tilde{v}(k), \tag{22}$$

$$Z_p(k)\tilde{v}(k) = -\tilde{p}(k; 0), \qquad Z_p(k) = \frac{1}{-\mathrm{i}\omega}(Dk^4 - m\omega^2). \tag{23}$$

The solution of equations (21) and (22) that represents either outward travelling waves or an exponentially decaying wavefield for $z \to \infty$—and thus meets the Sommerfeld radiation condition—is

$$\tilde{p}_{diff}(k; z) = Z_a(k)\tilde{v}(k) \exp(\mathrm{i}k_z z), \qquad Z_a(k) = \rho_0 \omega / k_z, \tag{24}$$

where the branch of the two-valued function $k_z = (k_0^2 - k^2)^{1/2}$ is chosen such that for real values of k

$$k_z = \begin{cases} |k_0^2 - k^2|^{1/2} & \text{for} \quad -k_0 < k < k_0; \\ \mathrm{i}|k^2 - k_0^2|^{1/2} & \text{for} \quad |k| > k_0. \end{cases} \tag{25}$$

Finally, the transforms of equations (16) and (17) can be found by recalling that these expressions are the solution of the Helmholtz equation (1) in free space with a point monopole source at $\underline{x}_s = (0, 0, \pm d)$, respectively. Taking the Fourier–Hankel transform of equation (1) and solving the transformed problem for the two source positions gives (details are given in the Appendix)

$$\tilde{p}_{inc}(k; z) = -q_s \frac{\exp[\mathrm{i}k_z|z-d|]}{2ik_z}, \qquad z > 0, \tag{26}$$

$$\tilde{p}_{spec}(k; z) = -q_s \frac{\exp[\mathrm{i}k_z(z+d)]}{2ik_z}, \qquad z > 0. \tag{27}$$

Solving equations (20), (23), (24), (26) and (27) for $\tilde{v}(k)$ and $\tilde{p}_{diff}(k; z)$ yields

$$\tilde{v}(k) = q_s \frac{\exp(\mathrm{i}k_z d)/ik_z}{Z_p(k) + Z_a(k)}, \tag{28}$$

$$\tilde{p}_{diff}(k; z) = q_s \frac{Z_a(k)}{Z_p(k) + Z_a(k)} \frac{\exp[\mathrm{i}k_z(d+z)]}{\mathrm{i}k_z}. \tag{29}$$

Inserting these expressions into the second form of the inverse transformation (19) gives the integral representations for $v(r)$ and $p_{diff}(r, z)$:

$$v(r) = \frac{q_s}{4\pi} \int_C \frac{\exp(\mathrm{i}k_z d)/\mathrm{i}k_z}{Z_p(k) + Z_a(k)} H_0^{(1)}(kr) k \, \mathrm{d}k, \tag{30}$$

$$p_{diff}(r, z) = \frac{q_s}{4\pi} \int_C \frac{Z_a(k)}{Z_p(k) + Z_a(k)} \frac{\exp[\mathrm{i}k_z(d+z)]}{\mathrm{i}k_z} H_0^{(1)}(kr) k \, \mathrm{d}k. \tag{31}$$

The total acoustic pressure $p(r, z)$ can be found by inserting expressions (16), (17) and (31) into formula (15).

In order to make the integral representations (30) and (31) suitable for numerical evaluation, the integrals are rewritten by means of the residue theorem. This procedure has been described elsewhere [14] for the line-driven plate (2D case). In the 3D case, however, the resulting expressions are singular for $r = 0$. This singularity can be avoided if one adopts an alternative choice for the representation of the pressure as given by Filippi [15]. For the present purpose, however, i.e., for the calculation of the imaginary part of the scattered pressure at the position of the source, it suffices to turn to the first form for the inverse transformation (19) and to evaluate this integral directly. This is done in the next section.

3.3. POWER OUTPUT OF THE SOURCE

In order to apply formula (9) the scattered pressure at the position of the source, i.e., $p_{scat}(\underline{x}_s)$, is evaluated as follows. First, it is noted that

$$p_{scat}(\underline{x}) = p_{spec}(\underline{x}) + p_{diff}(\underline{x}), \tag{32}$$

while

$$p_{spec}(\underline{x}_s) = q_s \frac{\exp(2ik_0 d)}{8\pi d}. \tag{33}$$

Inserting expression (29) into the first form of the inverse transformation (19) and specifying for $r = 0$ and $z = d$ gives

$$p_{diff}(\underline{x}_s) = \frac{q_s}{2\pi} \int_{C^+} \frac{Z_a(k)}{Z_p(k) + Z_a(k)} \frac{\exp(2ik_z d)}{ik_z} k \, dk. \tag{34}$$

Since k_0 is a branch point of k_z, the range of integration splits up naturally into two parts separated by k_0. Furthermore, it has been shown [16] that the denominator of the transform, i.e., $Z_p(k) + Z_a(k)$, has one real-valued, positive zero. This pole corresponds to an unattenuated, outgoing surface wave in the fluid and is coupled to a plate bending wave travelling along the plate towards infinity at subsonic speed. The pole is denoted by k_1 ($k_1 > \max\{k_0, k_p\}$ always holds; $k_p = (m\omega^2/D)^{1/4}$, see below) and is located on the contour of integration. Consequently, the Cauchy principal value of the integral must be taken while an additional residue contribution accounts for the presence of the pole. The contour of integration C^+ and the singularities of the integrand in the complex plane are shown in Figure 2. By writing down the various expressions it is easy to show that the residue contribution to $p_{diff}(\underline{x}_s)$ is purely imaginary, while the principal value integral over $k_0 < k < \infty$ is purely real. The integral over the finite range $0 < k < k_0$ is complex. This fits perfectly into the physical picture, since the pole corresponds to an outward travelling wave that carries energy away from the

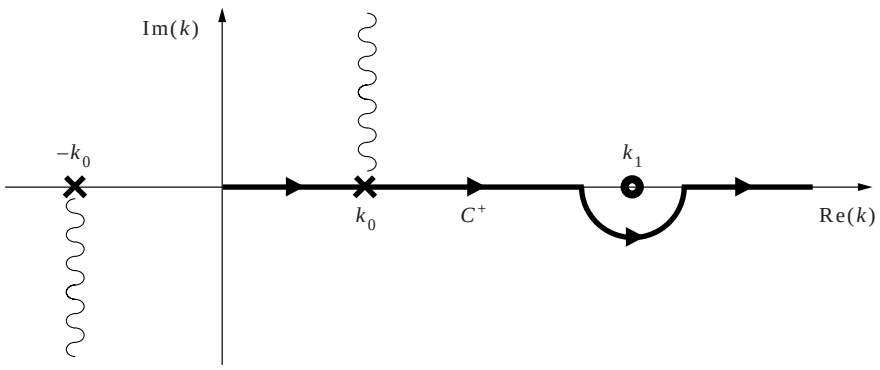

Figure 2. Contour of integration C^+, real-valued pole k_1 and branch points $\pm k_0$ in the complex k-plane.

source, while plate waves with subsonic wavenumbers cannot radiate effectively sound energy. The expression for $p_{diff}(\underline{x}_s)$ is

$$p_{diff}(\underline{x}_s) = \frac{\mathrm{i}}{2}\frac{q_s\rho_0}{m}\frac{\overline{k}_1}{4\overline{k}_1^3 + (\varepsilon/M)\overline{k}_1(\overline{k}_1^2 - M^2)^{-3/2}}\frac{\exp[-2k_p d(\overline{k}_1^2 - M^2)^{1/2}]}{(\overline{k}_1^2 - M^2)}$$

$$- \frac{1}{2\pi}\frac{q_s\rho_0}{m}\int_0^M \frac{\exp[2\mathrm{i}k_p d(M^2 - p^2)^{1/2}]}{(p^4 - 1)(M^2 - p^2)^{1/2} - \mathrm{i}\varepsilon/M}\frac{p\ \mathrm{d}p}{(M^2 - p^2)^{1/2}}$$

$$+ \frac{1}{2\pi}\frac{q_s\rho_0}{m}\,\mathrm{PV}\int_M^\infty \frac{\exp[-2k_p d(q^2 - M^2)^{1/2}]}{(q^4 - 1)(q^2 - M^2)^{1/2} - \varepsilon/M}\frac{q\ \mathrm{d}q}{(q^2 - M^2)^{1/2}}. \qquad (35)$$

In expression (35) all wavenumbers are normalized with respect to k_p, i.e., $\overline{k}_1 = k_1/k_p$, p, $q = k/k_p$ while the non-dimensional parameters ε and M are defined by

$$\varepsilon = \rho_0 c_0/m\omega_c, \qquad M = k_0/k_p = (\omega/\omega_c)^{1/2}. \qquad (36)$$

Here $k_p = (m\omega^2/D)^{1/4}$ is the plate bending wavenumber and $\omega_c = c_0^2(m/D)^{1/2}$ is the coincidence frequency. From equations (32), (33) and (35) the power delivered by the source can be found by using formula (9). The result is

$$\overline{\Pi} = \Pi/\Pi_\infty = 1 + \frac{\sin(2k_0 d)}{2k_0 d}$$

$$+ \frac{2\pi\varepsilon}{M^2}\frac{\overline{k}_1}{4\overline{k}_1^3 + (\varepsilon/M)\overline{k}_1(\overline{k}_1^2 - M^2)^{-3/2}}\frac{\exp[-2k_p d(\overline{k}_1^2 - M^2)^{1/2}]}{(\overline{k}_1^2 - M^2)}$$

$$- \frac{2\varepsilon}{M^2}\int_0^1 \frac{[M^4(1 - t^2)^2 - 1]t\sin(2k_0\,\mathrm{d}t) + (\varepsilon/M^2)\cos(2k_0\,\mathrm{d}t)}{[M^4(1 - t^2)^2 - 1]^2 t^2 + \varepsilon^2/M^4}\,\mathrm{d}t. \qquad (37)$$

It is noted that in order to simplify the integral the (dummy) integration variable has been changed from p to t by means of the successive transformations $p = M\cos\theta$ and $\sin\theta = t$.

3.4. FAR FIELD EXPRESSIONS AND RADIATED POWER

The acoustic energy emitted by the source is carried towards infinity by acoustic waves in the fluid and flexural waves in the plate. In this section the various power flows involved are evaluated directly from the far field expressions for the corresponding wavefields.

3.4.1. *Radiated acoustic power*

Upon introducing spherical co-ordinates (s, θ) by $r = s\sin\theta$, $z = s\cos\theta$, the far field expression for the acoustic pressure becomes

$$p(s, \theta) \sim \frac{\exp(\mathrm{i}k_0 s)}{s}D(\theta), \qquad 0 \leqslant \theta \leqslant \pi/2, \qquad s \to \infty, \qquad (38)$$

where $D(\theta)$ is the directivity function given by

$$D(\theta) = \frac{q_s}{4\pi} 2\cos(k_0 d\cos\theta) - \frac{\rho_0 \mathrm{i}\omega}{2\pi}\tilde{v}(k_0\sin\theta) \tag{39}$$

and $\tilde{v}(k)$ is given by equation (28). The first term in the formula for the directivity function follows straightforwardly from the incident and specularly reflected pressure fields, cf. reference [13]. The second term stems from the well-known relation between the directivity and the Fourier–Hankel transform of a plane velocity distribution; cf. reference [17]. Upon noting that $k_z(k_0\sin\theta) = k_0\cos\theta$ the directivity function reduces to

$$\frac{D(\theta)}{q_s/2\pi} = \cos(k_0 d\cos\theta) + \mathrm{i}\,\frac{\varepsilon}{M^2}\frac{\exp(\mathrm{i}k_0 d\cos\theta)}{(M^4\sin^4\theta - 1)\cos\theta - \mathrm{i}\varepsilon/M^2}. \tag{40}$$

The power radiated into the halfspace $z > 0$ can be found by integrating the far field acoustic intensity over a hemisphere at infinity, i.e.,

$$\Pi_{rad} = \lim_{s\to\infty}\frac{1}{2}\,\mathrm{Re}\left[\int_0^{2\pi}\mathrm{d}\phi\int_0^{\pi/2} s^2\sin\theta\,\mathrm{d}\theta p(s,\theta)\left\{\frac{1}{\rho_0\mathrm{i}\omega}\frac{\partial p}{\partial s}\right\}^*\right]$$

$$= \frac{\pi}{\rho_0 c_0}\int_0^{\pi/2} D(\theta)D^*(\theta)\sin\theta\,\mathrm{d}\theta.$$

Inserting the expression for $D(\theta)$ from (40), integrating the first term analytically and rewriting the integral by replacing the (dummy) integration variable θ by t according to $\cos\theta = t$ yields the following expression for the radiated acoustic power:

$$\bar{\Pi}_{rad} = \Pi_{rad}/\Pi_\infty = 1 + \frac{\sin(2k_0 d)}{2k_0 d}$$

$$- \frac{2\varepsilon}{M^2}\int_0^1 \frac{[M^4(1-t^2)^2 - 1]t\sin(2k_0\,\mathrm{d}t) + (\varepsilon/M^2)\cos(2k_0\,\mathrm{d}t)}{[M^4(1-t^2)^2 - 1]^2 t^2 + \varepsilon^2/M^4}\,\mathrm{d}t. \tag{41}$$

3.4.2. *Power flows along the plate*: *plate wave and surface wave*

In the previous section it was remarked that the pole k_1 is associated to a surface wave in the fluid that travels along the plate at subsonic speed accompanied by a flexural wave on the plate. The corresponding expressions for the acoustic pressure and the plate velocity can be obtained from equations (31) and (30) by closing the contour C by a semicircle at infinity in the upper halfplane and applying the residue theorem. The residue contribution of the pole k_1 gives the surface wave and its coupled counterpart on the plate. The other complex-valued pole(s) and the remaining integral along the branch cut of k_z do not contribute to this unattenuated wave, but to acoustic radiation as well as non-propagating near field

components. By turning to cylindrical co-ordinates (r, ϕ, z) the coupled field of the plate wave and surface wave can be represented in the form

$$v(r) \sim v_\infty H_0^{(1)}(k_1 r), \qquad r \to \infty \tag{42}$$

$$p(r, z) \sim p_\infty H_0^{(1)}(k_1 r) \exp[-(k_1^2 - k_0^2)^{1/2} z], \qquad r \to \infty, \tag{43}$$

where p_∞ and v_∞ are given by

$$v_\infty = -\frac{1}{2} \frac{q_s k_p}{m\omega} \frac{\overline{k}_1}{4\overline{k}_1^3 + (\varepsilon/M)\overline{k}_1(\overline{k}_1^2 - M^2)^{-3/2}} \frac{\exp[-k_p d(\overline{k}_1^2 - M^2)^{1/2}]}{(\overline{k}_1^2 - M^2)^{1/2}}, \tag{44}$$

$$p_\infty = \frac{i}{2} \frac{q_s \rho_0}{m} \frac{\overline{k}_1}{4\overline{k}_1^3 + (\varepsilon/M)\overline{k}_1(\overline{k}_1^2 - M^2)^{-3/2}} \frac{\exp[-k_p d(\overline{k}_1^2 - M^2)^{1/2}]}{(\overline{k}_1^2 - M^2)}, \tag{45}$$

It is noted that these expressions satisfy the condition (13) since

$$p_\infty / v_\infty = Z_a(k_1) = -\rho_0 \mathrm{i}\omega / (k_1^2 - k_0^2)^{1/2}.$$

The energy that is carried away by the surface wave in the fluid can be found by integrating the acoustic intensity over a cylindrical surface at infinity, i.e.,

$$\Pi_{sw,fl} = \lim_{r \to \infty} \frac{1}{2} \mathrm{Re} \left[\int_0^{2\pi} r \, \mathrm{d}\phi \int_0^\infty \mathrm{d}z p(r, z) \left\{ \frac{1}{\rho_0 \mathrm{i}\omega} \frac{\partial p}{\partial r} \right\}^* \right].$$

Upon inserting for p from expression (43) this becomes

$$\Pi_{sw,fl} = (p_\infty p_\infty^* / \rho_0 \omega) / (k_1^2 - k_0^2)^{1/2},$$

where the following properties of Hankel functions have been used:

$$\frac{\mathrm{d}}{\mathrm{d}r} H_0^{(1)}(k_1 r) = -k_1 H_1^{(1)}(k_1 r),$$

$$H_n^{(1)}(k_1 r) \sim \left(\frac{2}{\pi k_1 r} \right)^{1/2} \exp\left[\mathrm{i} \left(k_1 r - \frac{n\pi}{2} - \frac{\pi}{4} \right) \right], \qquad r \to \infty.$$

Inserting for p_∞ from equation (45) yields the expression for the power flow in the surface wave:

$$\overline{\Pi}_{sw,fl} = \Pi_{sw,fl} / \Pi_\infty = \frac{2\pi\varepsilon^2}{M^3} \frac{\overline{k}_1^2}{\{4\overline{k}_1^3 + (\varepsilon/M)\overline{k}_1(\overline{k}_1^2 - M^2)^{-3/2}\}^2} \frac{\exp[-2k_p d(\overline{k}_1^2 - M^2)^{1/2}]}{(\overline{k}_1^2 - M^2)^{5/2}}. \tag{46}$$

The elastic energy that propagates through the plate is found by integrating the elastic energy flux density, cf. reference [5], along a circle at infinity, i.e.,

$$\Pi_{sw,pl} = \lim_{r \to \infty} \frac{1}{2} \mathrm{Re} \left[\int_0^{2\pi} r \, \mathrm{d}\phi \, \frac{D}{-\mathrm{i}\omega} \left\{ \frac{\partial}{\partial r} (\Delta v) v^* - (\Delta v) \frac{\partial v^*}{\partial r} \right\} \right].$$

Upon using that $\Delta H_0^{(1)}(k_1 r) = -k_1^2 H_0^{(1)}(k_1 r)$, as well as the properties of Hankel functions mentioned above, it follows that

$$\Pi_{sw.pl} = 4(Dk_1^2/\omega)v_\infty v_\infty^*.$$

Inserting for v_∞ from equation (44) gives the result:

$$\bar{\Pi}_{sw.pl} = \Pi_{sw.pl}/\Pi_\infty = \frac{8\pi\varepsilon}{M^2} \frac{\bar{k}_1^4}{\{4\bar{k}_1^3 + (\varepsilon/M)\bar{k}_1(\bar{k}_1^2 - M^2)^{-3/2}\}^2} \frac{\exp[-2k_p d(\bar{k}_1^2 - M^2)^{1/2}]}{(\bar{k}_1^2 - M^2)}. \tag{47}$$

It is noted that the suffix *sw.pl* in expression (47) indicates that the plate wave is intimately coupled to the surface wave in the fluid. Actually, both waves cannot exist without supporting each other. The total energy that propagates along the plate to infinity (both in the fluid and in the plate) is

$$\bar{\Pi}_{sw} = \bar{\Pi}_{sw.fl} + \bar{\Pi}_{sw.pl} = \frac{2\pi\varepsilon}{M^2} \frac{\bar{k}_1}{4\bar{k}_1^3 + (\varepsilon/M)\bar{k}_1(\bar{k}_1^2 - M^2)^{-3/2}} \frac{\exp[-2k_p d(\bar{k}_1^2 - M^2)^{1/2}]}{(\bar{k}_1^2 - M^2)}. \tag{48}$$

It is easily verified that the following energy balance holds:

$$\bar{\Pi} = \bar{\Pi}_{rad} + \bar{\Pi}_{sw.fl} + \bar{\Pi}_{sw.pl}. \tag{49}$$

This relation states that all energy emitted by the source is carried to infinity by the various wave mechanisms of the fluid/plate system.

It is interesting to consider the low frequency limit of the ratio of the power flows in the plate and in the surface wave in the fluid, i.e.

$$\frac{\bar{\Pi}_{sw.fl}}{\bar{\Pi}_{sw.pl}} = \frac{1}{4}\frac{\varepsilon}{M}\frac{1}{\bar{k}_1^2(\bar{k}_1^2 - M^2)^{3/2}}. \tag{50}$$

At low frequencies the following asymptotic relations hold:

$$k = k_1 \gg k_0, \quad \text{so} \quad \bar{k}_1 \gg M, \tag{51}$$

$$k = k_1 \gg k_p, \quad \text{so} \quad \bar{k}_1 \gg 1. \tag{52}$$

Consequently, the dispersion relation $Z_p(k_1) + Z_a(k_1) = 0$ reduces to

$$\frac{Dk_1^4}{-i\omega} + \frac{\rho_0\omega}{ik_1} = 0, \quad \text{so} \quad \bar{k}_1^5 = \frac{\varepsilon}{M}. \tag{53}$$

Using inequality (51) and subsequently inserting for $\bar{k}_1$ from equation (53) yields

$$\frac{\bar{\Pi}_{sw.fl}}{\bar{\Pi}_{sw.pl}} \sim \frac{1}{4}. \tag{54}$$

This result is due to Krasil'nikov [5] and is fully confirmed by the numerical results presented in the next section.

4. NUMERICAL RESULTS AND DISCUSSION

All numerical results that are presented here were obtained for the case of steel plates in water. This choice determines the value of ε which was taken $\varepsilon = 0{\cdot}132$.

The other non-dimensional parameters that appear in the expressions for the various power flows are M, $k_0 d$ and $k_p d$, all being frequency dependent. However, only two parameters can be chosen independently, since $M = k_0 d/k_p d$. In addition, it is advantageous to have only one frequency parameter. Therefore, a different combination of parameters is chosen in this paper, namely $k_0 d$ and h/d. The Helmholtz number $k_0 d$ is the frequency parameter containing the frequency of the incident wave as well as the distance d, while h/d is a geometrical parameter containing the plate thickness h. It is noted that

$$\frac{h}{d} = \frac{\omega_c h}{c_0} \frac{M^2}{k_0 d}, \tag{55}$$

where $\omega_c h/c_0 = \varepsilon^{-1}\rho_0/\rho_p = 0{\cdot}966$ for steel plates in water. Except for the special case $d = 0$ the various power flows vary with both $k_0 d$ and h/d and the aim of this section is to investigate these variations, i.e., the dependencies of the power flows upon $k_0 d$ and h/d, by presenting numerical results for a wide range of values in this two-dimensional parameter space.

For the case of a point source placed directly on the plate, i.e., $d = 0$, the results depend on one parameter only, but neither $k_0 d$ nor h/d is a suitable choice for this case. A convenient choice for the frequency parameter is M as given by equation (36). Inserting $d = 0$ in expressions (37), (41), (46) and (47) gives the various power flows for this case. The results are presented in Figure 3. At low frequencies ($M \ll 1$) all energy emitted by the source is transmitted to infinity by the surface wave and its plate companion, while at higher frequencies radiation becomes more important. Actually, for frequencies well above coincidence ($M \gg 1$) radiation becomes the dominating mechanism of power transmission to infinity. These qualitative features are characteristic for fluid-loading and may be summarized as follows: $\bar{\Pi} \to \bar{\Pi}_{sw}$ and $\bar{\Pi}_{rad} \to 0$ for $M \to 0$, while $\bar{\Pi} \to \bar{\Pi}_{rad}$ and $\bar{\Pi}_{sw} \to 0$ for $M \to \infty$.

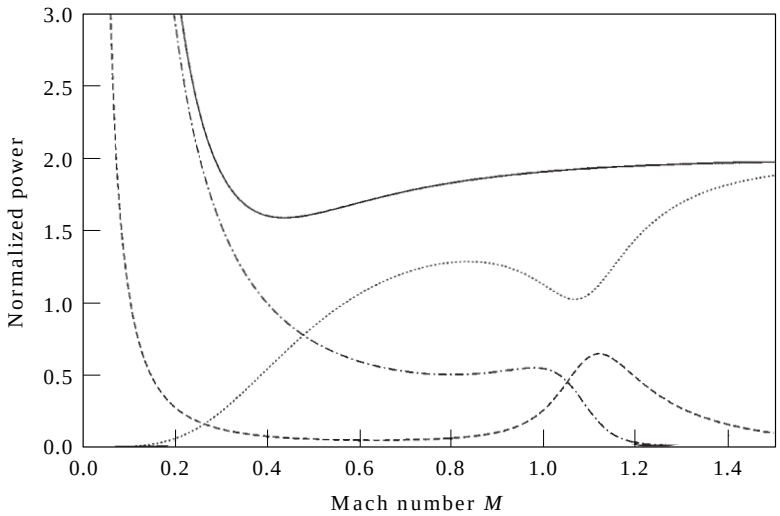

Figure 3. Normalized power flows for monopole sound source on fluid-loaded plate ($d = 0$) versus frequency parameter M. Solid line, total power output $\bar{\Pi}$; dotted line, radiated power $\bar{\Pi}_{rad}$; dash-dot line, power flow in surface wave $\bar{\Pi}_{sw,fl}$; dashed line, power flow through plate $\bar{\Pi}_{sw,pl}$.

Moreover, $\bar{\Pi} \to 2$ for $M \to \infty$, which is the value for a point source on a rigid wall, according to formula (11). This means that the plate is not excited at high frequencies and thus behaves like a rigid wall. At low frequencies, however, the plate is excited considerably and $\bar{\Pi}$ becomes unbounded, while the radiated power $\bar{\Pi}_{rad}$ goes to zero as in the case of a free surface. This comparison is not unreasonable because the plate is highly compliant to the incident pressure at low frequencies.

In the neighbourhood of coincidence, i.e., for $M \approx 1$, a dip appears in the radiated power, while the power flow in the surface wave shows a peak here and the power flow through the plate drops to zero rapidly. This behaviour is typical for frequencies in the coincidence range and also shows up in the case of a fluid-loaded plate excited by a localized mechanical forcing like a point force, a line force or a line moment. Although there is a considerable redistribution of energy among the three transmission paths, which involves about 30% of the total energy, it is noted that the total power output changes only gradually and is not affected on passage through coincidence.

For the case of a point source at finite, non-zero distance from the plate ($d \neq 0$) numerical results for the various power flows were obtained for parameter values ranging from $0{\cdot}001 \leqslant h/d \leqslant 1{\cdot}0$ and $10^{-2} \leqslant k_0 d \leqslant 10$. In Figures 4–7 the power flows are presented as a function of the frequency parameter $k_0 d$ for $h/d = 1{\cdot}0$, $0{\cdot}1$, $0{\cdot}01$ and $0{\cdot}001$, respectively. For comparison and easy reference the radiated power for the case of a point source at distance d below a pressure release surface has been included as well. It is observed that the results show the typical structure which is characteristic for fluid-loading: at low frequencies, i.e., for $k_0 d \ll 1$, all energy emitted by the source is transferred to the plate wave and its subsonic surface wave comparison in the fluid, while at high frequencies ($k_0 d \gg 1$) acoustic

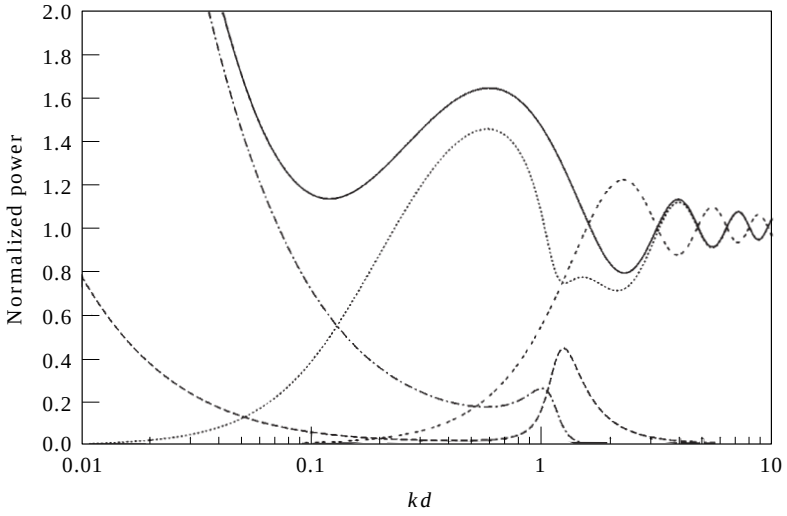

Figure 4. Normalized power flows for monopole sound source near fluid-loaded plate ($h/d = 1{\cdot}0$) versus frequency parameter $k_0 d$. Solid line, total power output $\bar{\Pi}$; dotted line, radiated power $\bar{\Pi}_{rad}$; dash-dot line, power flow in surface wave $\bar{\Pi}_{sw,fl}$; dashed line, power flow through plate $\bar{\Pi}_{sw,pl}$; doubly dashed line, power output of source at distance d below free surface.

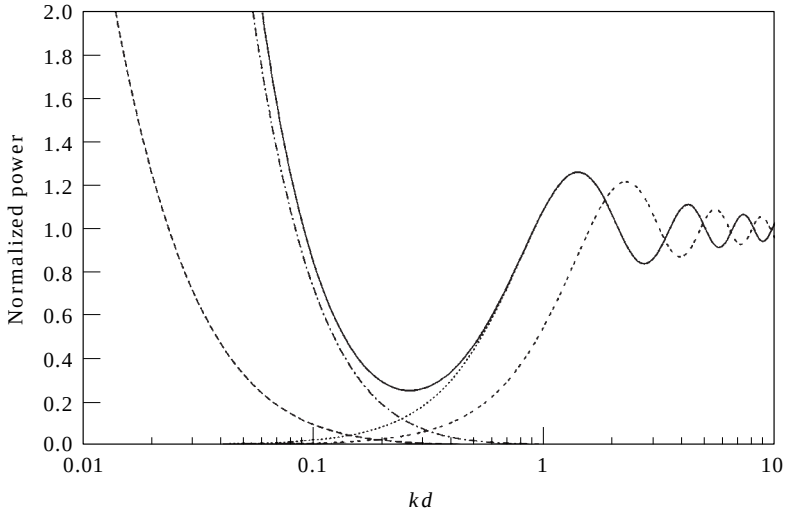

Figure 5. As Figure 4 but for $h/d = 0{\cdot}1$.

radiation dominates the transmission of energy from the source to infinity. It is also observed that in some intermediate region $\bar{\Pi}_{sw}$ balances $\bar{\Pi}_{rad}$. However, the break-even point depends on the value of h/d and runs from $k_0 d \approx 0{\cdot}017$ for $h/d = 0{\cdot}001$ to $k_0 d \approx 0{\cdot}25$ for $h/d = 0{\cdot}1$ and back to $k_0 d \approx 0{\cdot}11$ for $h/d = 1{\cdot}0$. Moreover, the power output by the source attains its minimum for values of $k_0 d$ close to this break-even point. Detailed numerical results for the total power output of the source as a function of both $k_0 d$ and h/d are presented at the end of this section. For $k_0 d \gg 1$ the radiated power $\bar{\Pi}_{rad}$ approaches the freefield value, which is 1, but also shows the typical modulation effect due to the finite distance from the source to the plate. For $h/d = 1{\cdot}0$ and $0{\cdot}1$ this modulation is comparable to that for a perfectly rigid wall, while for $h/d = 0{\cdot}01$ and $0{\cdot}001$ the modulation

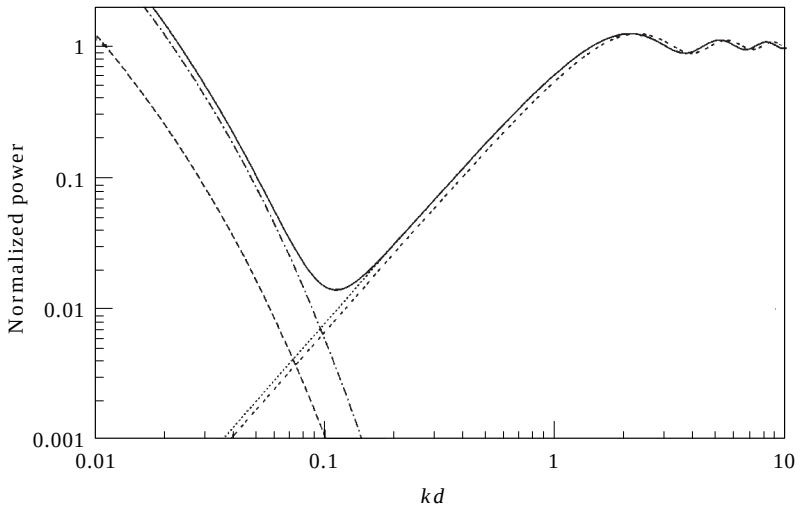

Figure 6. As Figure 4 but for $h/d = 0{\cdot}01$.

effect is close to that for a free surface. On the other hand, at low frequencies, it is evident from Figures 4–7 that $\bar{\Pi}_{sw} \to \infty$ for $k_0 d \to 0$, while it is noted that Krasil'nikov's asymptotic result (54) is confirmed numerically. Additionally, $\bar{\Pi}_{rad} \to 0$ for $k_0 d \to 0$. The latter result can be put more precisely as follows: $\bar{\Pi}_{rad} = \mathcal{O}((k_0 d)^2)$ for $k_0 d \to 0$. For $h/d = 0{\cdot}01$ and $0{\cdot}001$ the numerical constant in this asymptotic relationship goes to 2/3, i.e., $\bar{\Pi}_{rad} \to \frac{2}{3}(k_0 d)^2$, which is the low frequency limit for the pressure release surface, according to formula (11). Nevertheless, the trend $\bar{\Pi}_{rad} = \mathcal{O}((k_0 d)^2)$ is also present for higher values of h/d, as can be seen from Figures 4 and 5. This is the reason to refer to this low frequency behaviour as a *free surface* effect. Actually, this description is physically correct, because the plate behaves like a pressure release surface, which, by definition, is called a free surface.

Figure 4 also shows a redistribution of energy among the various transmission paths for frequencies close to coincidence, i.e., for $M = 1$, which corresponds to $k_0 d \approx 1{\cdot}03488$ for $h/d = 1{\cdot}0$. This redistribution involves about 25% of the total energy in the system. The total power output of the source, however, shows no dips or peaks at coincidence.

Finally, the total power output of the source was calculated for the full range of parameters $0{\cdot}001 \leqslant h/d \leqslant 1{\cdot}0$ and $10^{-2} \leqslant k_0 d \leqslant 10$. The results are presented in Figure 8. In this figure, equal level contour lines are drawn for the total power output of the source. The spacing between two adjacent lines is approximately 3·05 dB and ranges from $-36{\cdot}2$ dB at $(k_0 d,\ h/d) = (0{\cdot}0166,\ 0{\cdot}001)$ to $+12{\cdot}7$ dB at $(k_0 d,\ h/d) = (0{\cdot}01,\ 0{\cdot}0646)$. Since the absolute value of $\bar{\Pi}$ ranges over five decades, the modulation effect, for $k_0 d \geqslant 1$, cannot be made visible on this scale, so the results in Figure 8 were restricted to the region $k_0 d \leqslant 1$. Both parameter axes in Figure 8 have logarithmic scaling, so M is constant along the straight lines

$$\log_{10}(k_0 d) + \log_{10}(h/d) = \log_{10}(\omega_c h/c_0) + 2\log_{10}(M) = \text{constant},$$

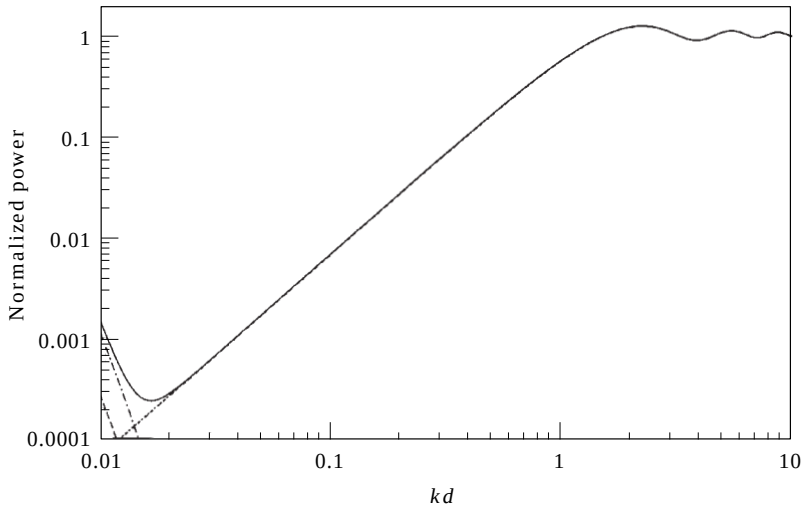

Figure 7. As Figure 4 but for $h/d = 0{\cdot}001$.

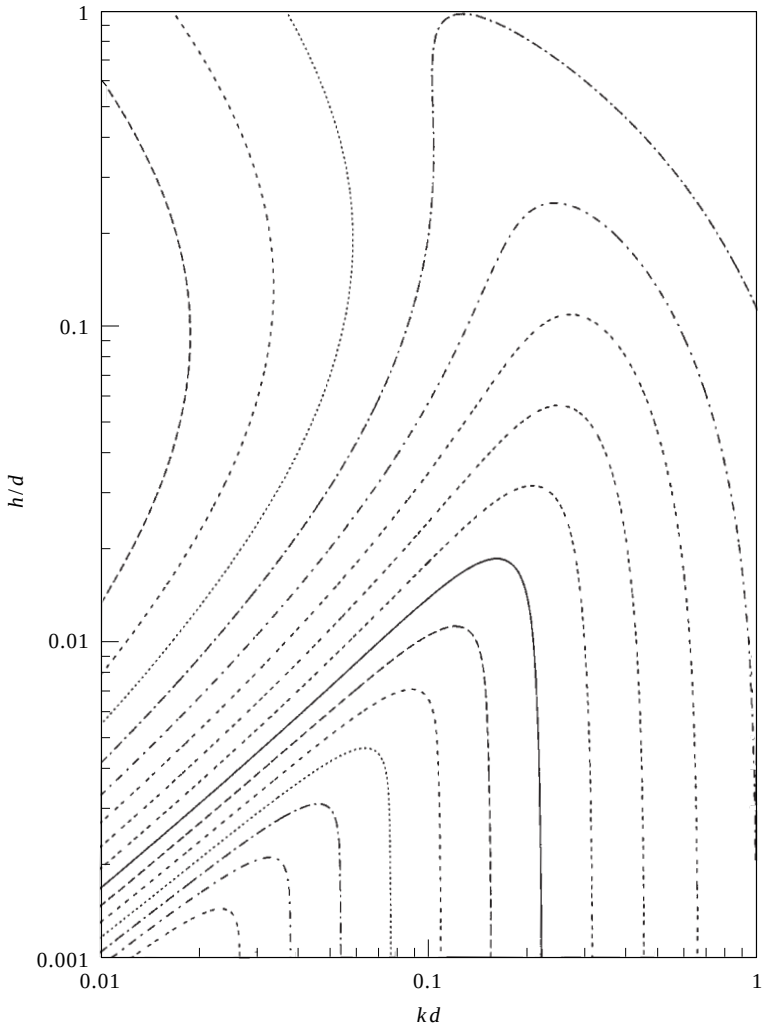

Figure 8. Equal level contour lines for total power output $10 \log_{10} \bar{\Pi}$ as a function of frequency parameter $k_0 d$ and geometrical parameter h/d. Spacing between adjacent lines is 3·05 dB and runs from $-36{\cdot}2$ dB at $(k_0 d,\ h/d) = (0{\cdot}0166,\ 0{\cdot}001)$ to $+12{\cdot}7$ dB at $(k_0 d,\ h/d) = (0{\cdot}01,\ 0{\cdot}0646)$.

which follows from relation (55). Upon recalling that $\omega_c h/c_0 = 0{\cdot}966$ for steel plates in water, it is easy to verify that M^2 runs from 10^{-5} for $(k_0 d,\ h/d) = (0{\cdot}01,\ 0{\cdot}001)$ to 1 for $(k_0 d,\ h/d) = (1{\cdot}0,\ 1{\cdot}0)$.

Concerning the region $k_0 d \geqslant 1$, which is *not* shown in Figure 8, the total power is determined mainly by the radiated power and shows the typical modulation effect due to the finite distance from the source to the plate. Referring to the discussion of Figures 4–7, it was remarked that for $h/d \geqslant 0{\cdot}1$ this modulation effect is similar to that for a rigid wall, while for $h/d \leqslant 0{\cdot}01$ it resembles that for a free surface. However, the parameter that controls the transition of the modulation

effect from the free surface case to the rigid wall limit appears to be M^2 rather than h/d. Therefore, this observation can be put more precisely as follows: for $M^2 = \mathcal{O}(1)$ and larger, the modulation effect of the plate is similar to that of a rigid wall and for $M^2 \ll 1$ the effect of the plate is like a perfectly compliant surface.

In the triangular region $k_0 d \leqslant 1$ and $h/d \leqslant \frac{1}{20} k_0 d$ the results do not vary significantly with h/d, but the power output increases with $k_0 d$ at a constant rate of 20 dB/decade. This behaviour has been discussed before: in connection with Figures 4–7 it was observed that $\bar{\Pi}_{rad} = \mathcal{O}((k_0 d)^2)$ for $k_0 d \to 0$ and this trend was called the free surface effect. Indeed, the radiated power still dominates the power output of the source and the plate behaves like a pressure release surface.

Finally, in a third region, i.e., for $0{\cdot}1 > h/d > \frac{1}{10} k_0 d$ the contour lines are all parallel to each other and perpendicular to the lines $M^2 = \text{constant}$. In this region the power output is independent of M, but increases strongly with decreasing values of $k_0 d^2/h$. It is noted, however, that the radiated power is very small compared to the power output of the source, while almost all energy emitted by the source is carried to infinity by the power flows along the plate. So, although the radiated power coincides with the free surface case and the plate is very compliant to the incident pressure, the total power output of the source increases dramatically to orders of magnitude above the freefield value. This is due to the strong excitation of the plate in this parameter region.

The equal level contour lines in Figure 8 can be used to select those parameter values for $k_0 d$ and h/d which minimize the total power output of the source. However, designers of ships have to conform to other, non-acoustical requirements as well. For many ships, the parameter $k_0 d$, where k_0 is based on the fifth harmonic of the blade passage frequency, has a value within the range† $0{\cdot}37 \leqslant k_0 d \leqslant 0{\cdot}45$. This type of correlation between k_0 and d is to be expected, since large propellers operate at low r.p.m. numbers and conversely, small propellers operate at higher frequencies. It is noted that for sheet cavitation the source spectrum has a peak value at the fourth or fifth harmonic of the blade passage frequency, while the center of cavitation is taken at aobut 0·8–0·9 radii above the propeller axis. The results from Figure 8 indicate that for $k_0 d \approx 0{\cdot}40$ the power output of the source is independent of the value of h/d as long as this parameter not exceeds the value 0·1.

It is noted, however, that this conclusion is based on the underlying model of a point source below an infinite, homogeneous plate. This model does not account for resonances that occur due to the finiteness of hullplates of ships. Therefore, in certain frequency ranges, resonant vibrations of hullplates can greatly disrupt the structure of the power output of the source from the one given in Figure 8. This issue has been addressed in a separate study [18].

† M.J.A.M. de Regt, TNO Institute of Applied Physics, private communication.

ACKNOWLEDGMENTS

The author is indebted to Dr Ir. C. A. F. de Jong for converting the numerical data into the contour plot (Figure 8). Data on several ships were kindly provided by Mr M. J. A. M. de Regt. Valuable comments on an earlier draft of the manuscript were given by Dr Ir. A. H. P. van der Burgh. This work was supported by the TNO Institute of Applied Physics, Delft, The Netherlands.

REFERENCES

1. J. VAN DER KOOIJ 1986 in *Proceedings of the 2nd International Symposium on Shipboard Acoustics* (J. Buiten, editor) 43–62. Dordrecht: Martinus Nijhoff. Experimental and analytical aspects of propeller induced pressure fluctuations.
2. J. C. BRUGGEMAN and A. HUISMAN 1988 in *Proceedings of the SNAME Propellers '88 Symposium*, 4–1/4–18. New York: SNAME. Acoustic performance of the highly skewed propeller of a ro-ro container ship.
3. J. BUIST and H. C. RAVEN 1991 in *Cavitation and Multiphase Flow Forum*—1991, *Proceedings of the 1st ASME/JSME Fluids Engineering Conference*, FED-Vol. 109 (O. Furuya and H. Kato, editors), 171–175. New York: ASME. A consistently linearized approach for the calculation of partial sheet cavitation.
4. T. TEN WOLDE and A. DE BRUIJN 1975 *International Shipbuilding Progress* **22**, 385–396. A new method for the measurement of the acoustical source strength of cavitating ship propellers.
5. V. N. KRASIL'NIKOV 1960 *Soviet Physics Acoustics* **6**, 216–224. Effect of a thin elastic layer on the propagation of sound in a liquid halfspace.
6. G. H. SCHMIDT 1977 *Journal of Sound and Vibration* **53**, 289–300. Influence of an unbounded elastic plate on the radiation of sound by a point source.
7. H. SAADAT and P. FILIPPI 1981 *Journal of the Acoustical Society of America* **69**, 397–403. Diffraction of a spherical wave by a thin, infinite plate.
8. M. HECKL 1969 *Acustica* **21**, 149–161. Körperschallanregung von elastischen Strukturen durch benachbarte Schallquellen.
9. J. W. S. RAYLEIGH 1945 *The Theory of Sound* **II**. New York: Dover; second edition. See section 319, pp. 211–214.
10. W. VAN GENT, G. A. Q. SALVATI and H. C. J. VAN WIJNGAARDEN 1989 in *Proceedings of the ASME International Symposium Cavitation, Noise and Erosion in Fluid Systems*, FED-Vol. 88 (R. E. A. Arndt, M. L. Billet and W. K. Blake, editors) 19–27. New York: ASME. Response of elastic flat plate to cavitation.
11. A. DE BRUIJN 1991 *Nederlands Akoestisch Genootschap Journaal* **110**, 53–63. Akoestisch gedrag van onderwatergeluidbronnen in de nabijheid van elastische structuren. (In Dutch).
12. A. DE BRUIJN 1992 in *Proceedings of Underwater Defense Technology* (B. R. Longworth, editor) 134–140. London: Microwave Exhibitions and Publishers. Acoustical behavior of underwater sound sources near compliant layers.
13. A. D. PIERCE 1989 *Acoustics. An Introduction to its Physical Principles and Applications*. New York: ASA/AIP; second edition. See chapter 5, p. 212.
14. P. R. NAYAK 1970 *Journal of the Acoustical Society of America* **47**, 191–201. Line admittance of infinite isotropic fluid-loaded plates.
15. P. J. T. FILIPPI 1983 *Journal of Sound and Vibration* **91**, 65–84. Extended sources radiation and Laplace type integral representation: application to wave propagation above and within layered media.
16. D. G. CRIGHTON 1979 *Journal of Sound and Vibration* **62**, 225–235. The free and forced waves on a fluid-loaded elastic plate.
17. M. C. JUNGER and D. FEIT 1986 *Sound, Structures and Their Interaction*. Cambridge: MIT-Press; second edition. See chapter 5, pp. 92–105.

18. C. KAUFFMANN 1998 *Journal of the Acoustical Society of America* **104,** 3245–3250. Efficiency of a monopole sound source in the vicinity of an elastically suspended, baffled disk.

APPENDIX: FOURIER-HANKEL TRANSFORM OF THE FREE SPACE GREEN FUNCTION

In this appendix the Fourier–Hankel transform is derived of the solution of the Helmholtz equation in free space with a point monopole source at the origin. Starting by transforming equation (1) with $\underline{x}_s = \underline{0}$ gives

$$\left\{\frac{\mathrm{d}^2}{\mathrm{d}z^2} + (k_0^2 - k^2)\right\}\tilde{p}(k; z) = -q_s\,\delta(z). \tag{56}$$

A general solution of equation (56) for $z \neq 0$ is

$$\tilde{p}(k; z) = A_{\pm}\exp(\mathrm{i}k_z z) + B_{\pm}\exp(-\mathrm{i}k_z z), \tag{57}$$

where the $\pm$ signs correspond to $z > 0$ and $z < 0$, respectively. The appropriate branch of the two-valued function $k_z = (k_0^2 - k^2)^{1/2}$ is specified by formula (25). In order to satisfy the radiation condition for $z \to \pm\infty$ it is required that $A_- = 0$ and $B_+ = 0$. Furthermore, from symmetry considerations, it follows that $A_+ = B_- \equiv A$. The value of A is chosen such that the solution satisfies equation (56) for $z = 0$ as well. This is accomplished by integrating both sides of equation (56) over the range $-\triangle \leqslant z \leqslant \triangle$. Invoking the well-known filter property from the definition of the delta function the right-hand-side becomes

$$\int_{-\triangle}^{\triangle} -q_s\,\delta(z)\,\mathrm{d}z = -q_s.$$

The left-hand-side can be evaluated by using integration by parts. This gives

$$\int_{-\triangle}^{\triangle}\left\{\frac{\mathrm{d}^2}{\mathrm{d}z^2} + k_z^2\right\}\tilde{p}\,\mathrm{d}z = \left[\frac{\mathrm{d}\tilde{p}}{\mathrm{d}z}\right]_{-\triangle}^{\triangle} + k_z^2\int_{-\triangle}^{\triangle}\tilde{p}\,\mathrm{d}z$$

$$= A_+\mathrm{i}k_z\exp(\mathrm{i}k_z\triangle) - B_-\cdot -\mathrm{i}k_z\exp(-\mathrm{i}k_z\cdot -\triangle) + k_z^2\int_{-\triangle}^{\triangle}\tilde{p}\,\mathrm{d}z.$$

Taking the limit for $\triangle \to 0$ and using that $\tilde{p}$ is finite and continuous at $z = 0$ yields $-q_s = (A_+ + B_-)\mathrm{i}k_z$ so $A = -q_s/2\mathrm{i}k_z$. Combining the results for both $z > 0$ and $z < 0$ it follows that $\tilde{p}$ is given by

$$\tilde{p}(k; z) = -q_s\frac{\exp(\mathrm{i}k_z|z|)}{2\mathrm{i}k_z}. \tag{58}$$

Finally, for the case of a point source at the z-axis which is not located at $\underline{x}_s = \underline{0}$, expression (58) is easily modified by a simple shift of the origin.